Pergamon

Planet. Space Sci., Vol. 44, No. 2, pp. 129–135, 1996

0032-0633/96 $15.00+0.00

0032–0633(95)00083–6

Alfvén modes in dusty cometary and planetary plasmas

R. V. Reddy,[1] G. S. Lakhina,[1] Frank Verheest[2] and Peter Meuris[3]

[1] Indian Institute of Geomagnetism, Dr Nanabhai Moos Marg, Colaba, Bombay 400005, India
[2] Sterrenkundig Observatorium, Universiteit Gent, Krijgslaan 281, B-9000 Gent, Belgium
[3] Belgisch Instituut voor Ruimte-Aëronomie, Ringlaan 3, B-1180 Ukkel, Belgium

Received 6 March 1995; revised 22 May 1995; accepted 1 June 1995

Abstract. Dusty plasmas contain charged dust grains which are much bigger than protons and usually carry high negative charges owing to preferential capture of electrons. These dust grains do not have a fixed charge, and perturbations in the plasma induce fluctuations in the grain charges owing to liberation or capture of additional electrons and protons. The dispersion relation for low-frequency, long-wavelength and non-resonant electromagnetic fluctuations in a multibeam dusty plasma is derived by taking into account the momentum loss of electrons and protons owing to dust charge fluctuations. When the charging and discharging effects conserve momentum between any two species, the modes become unstable provided that a normalized averaged drift velocity exceeds the Alfvén velocity. However, when the charging and discharging effects are more complicated, drift dissipative type modes are excited when the normalized averaged drift velocity is below the Alfvén velocity. These modes could generate spatial structures over a wide range from hundreds to tens of millions of kilometres in dusty cometary tails. The analysis could be applied to certain planetary rings and to a dusty interstellar medium.

1. Introduction

Dusty plasmas are observed in several astro and space physical environments such as nebulas, cometary environments, planetary rings, planetary magnetospheres, etc. (Spitzer, 1978; Goertz, 1989). The dust grains in these dusty plasmas are usually highly charged owing to various processes, including plasma currents, photoemission, secondary emission, field emission, etc. (Draine and Salpeter, 1979). The presence of these massive, highly charged dust particles may significantly influence various physical processes in dusty plasmas (Goertz, 1989; Mendis and Rosenberg, 1994).

Electrostatic waves in dusty plasmas have been studied by several workers (Havnes, 1988; de Angelis *et al.*, 1988; Rao *et al.*, 1990; Shukla *et al.*, 1991, Verheest, 1992a), treating the dust charge as constant.

In a dusty plasma, momentum loss of electrons, protons and dust particles can occur because of collisions or fluctuations in the dust charges. The sticking or loosening of electrons or protons on and off dust grains may significantly affect the charge to mass ratio of dust particles. In contrast to multi-ion plasma systems where each ion species has a fixed charge number, in dusty plasmas the charge on the dust grains can change continuously owing to fluctuations in the plasma currents that flow to the dust grains. Hence, for electron or ion oscillations, charge density fluctuations are number density fluctuations only; we see that for the dust grains, number densities as well as charges could change owing to the wave.

The effects of the variation of the charge on the dust grain owing to the wave field of electrostatic dust-acoustic instabilities have been studied (Melandsø *et al.*, 1993a,b; Varma *et al.*, 1993; Jana *et al.*, 1993; Bhatt and Pandey, 1994; D'Angelo, 1994; Li *et al.*, 1994). It is found that dust charge fluctuations lead to damping of the dust-acoustic modes because of phase differences between the wave potential and the dust charge.

Low-frequency, long-wavelength, nonresonant electromagnetic fluctuations in multi-beam plasmas were studied to explain the Alfvén wave turbulence in the plasma sheet boundary layer of Earth's magnetotail and in cometary environments (Lakhina, 1987; Verheest, 1987; Lakhina and Verheest, 1988; Gary and Winske, 1990; Galeev *et al.*, 1991; Verheest and Lakhina, 1991).

Charged dust grains can also affect electromagnetic modes by substantially lowering the Alfvén speed (Shukla, 1992; Shukla and Stenflo, 1992). The linear and nonlinear evolution of various low-frequency electromagnetic modes in dusty plasmas have been discussed recently (Shukla, 1992; Verheest, 1992b; Verheest and Buti, 1992; Rao, 1993), treating the dust charge as constant, however.

Correspondence to: F. Verheest

The aim of our paper is to study low-frequency, long-wavelength, nonresonant electromagnetic fluctuations in a three component multi-beam dusty plasma by taking account of the momentum loss of electrons, protons and dust grains. Sink/source terms have been added in the continuity and momentum equations to make the analysis self-consistent, elaborating on earlier ideas (Verheest, 1994; Verheest and Meuris, 1995). In addition, the dust dynamics are now also taken into account, rather than considering the dust as a neutralizing background with fluctuating charges as we did before (Verheest and Meuris, 1995).

The structure of our paper is as follows. In Section 2 we recall and discuss the model equations used, from which we derive in Section 3 the dispersion law for electromagnetic modes in the low-frequency, long-wavelength limit. Different possibilities for this dispersion law are discussed in Section 4, and in Section 5 we conclude by giving some relevant estimates for cometary dusty plasmas and pointing out the possible relevance for certain planetary plasmas.

2. Methodology

We consider a homogeneous multi-beam dusty plasma immersed in a uniform magnetic field, $\mathbf{B}_0 = B_0\mathbf{e}_z$. The multi-beam dusty plasma consists of electrons, protons, and dust particles. For simplicity, we restrict ourselves to wave propagation parallel to $\mathbf{B}_0$. The treatment holds good for both cold and warm plasmas, as long as the pressure anisotropies can be neglected. The electromagnetic fluctuations of the nonlinear multi-beam dust Alfvén waves, taking into account the charge fluctuations and momentum losses of ions, electrons and dust particles, may be described by the following basic equations, writing only those we will explicitly need:

$$\left(\frac{\partial}{\partial t}+\mathbf{u}_\alpha\cdot\nabla\right)\mathbf{u}_\alpha = \frac{q_\alpha}{m_\alpha}(\mathbf{E}+\mathbf{u}_\alpha\times\mathbf{B})-\sum_\beta \gamma_{\alpha\beta}(\hat{\mathbf{u}}_\alpha-\hat{\mathbf{u}}_\beta) \quad (1)$$

$$\nabla\times\mathbf{E}+\frac{\partial}{\partial t}\mathbf{B} = 0 \quad (2)$$

$$c^2\nabla\times\mathbf{B} = \frac{\partial}{\partial t}\mathbf{E}+\frac{1}{\varepsilon_0}\sum_\alpha n_\alpha q_\alpha \mathbf{u}_\alpha. \quad (3)$$

In these equations n_α, m_α, q_α and $\mathbf{u}_\alpha$ respectively refer to the number density, mass, charge and fluid velocity per species, labelled with subscript α, $\mathbf{E}$ and $\mathbf{B}$ to the electric and magnetic fields, and c to the speed of light. Source or sink terms have been included to account for the momentum losses or gains of the species owing to fluctuations in the charges of the dust grains, which liberate or capture electrons and protons. In equation (1) the hat over the variables indicates that only the deviations from the equilibrium values are taken into account. These deviations need not be especially small, but in equilibrium the dust grains are supposed to be charged to a certain extent, and their charges will remain constant as long as nothing perturbs the plasma.

The form of the mass and momentum exchanges have been inspired by what is usually written for ordinary collisional exchanges (Booker, 1984; Pilipp *et al.*, 1987; Verheest and Meuris, 1995). It should be emphasized that ideally the coefficients $\gamma_{\alpha\beta}$ characterizing the source or sink terms should be computed from an appropriate and self-consistent kinetic theory, which is, however, not yet available. For the time being we will be content to help ourselves with these *ad hoc* coefficients, introduced to illustrate what can happen when momentum gains or losses are taken into account for the different species.

With the indices e, i and d we will refer to electrons, ions (usually protons assumed here to be singly charged) and average dust grains. So in the momentum equations (1) for the electrons or the ions the sum over β is restricted to the interfacing with the dust, hence we find terms in γ_{ed} or γ_{id} only. On the contrary, for the dust there will be terms both with γ_{de} and γ_{di}.

3. Electromagnetic modes

We define $n_\alpha = n_{\alpha 0}+\delta n_\alpha$, $\mathbf{E} = \delta\mathbf{E}$, $\mathbf{u}_\alpha = u_{\alpha 0}\mathbf{e}_z+\delta\mathbf{u}_\alpha$, and $\mathbf{B} = B_0\mathbf{e}_z+\delta\mathbf{B}$. The subscript 0 represents the physical quantities at their equilibrium state and δ represents their first-order perturbations. The perturbations themselves are assumed to be of the form $\delta f = f_1 \exp i(kz-\omega t)$, where $\mathbf{k} = k\mathbf{e}_z$ is the wave vector. Linearizing (1)–(3), we obtain for the zeroth order that

$$\sum_\alpha n_{\alpha 0}q_{\alpha 0} = 0, \quad \sum_\alpha n_{\alpha 0}q_{\alpha 0}u_{\alpha 0} = 0. \quad (4)$$

To first order we obtain for transverse modes that

$$(\omega-ku_{\alpha 0})\mathbf{u}_{\alpha 1}+i\Omega_\alpha\mathbf{e}_z\times\mathbf{u}_{\alpha 1} +i\sum_\beta \gamma_{\alpha\beta}(\mathbf{u}_{\alpha 1}-\mathbf{u}_{\beta 1}) = i\frac{q_{\alpha 0}(\omega-ku_{\alpha 0})}{\omega m_\alpha}\mathbf{E}_1 \quad (5)$$

$$\mathbf{k}\times\mathbf{E}_1 = \omega\mathbf{B}_1 \quad (6)$$

$$ic^2\mathbf{k}\times\mathbf{B}_1 = \frac{1}{\varepsilon_0}\sum_\alpha n_{\alpha 0}q_{\alpha 0}\mathbf{u}_{\alpha 1}-i\omega\mathbf{E}_1. \quad (7)$$

We will now look at circularly polarized, low-frequency and long-wavelength modes such that

$$\left|\frac{\gamma_{\alpha\beta}}{\Omega_\alpha}\right| \sim \left|\frac{\omega-ku_{\alpha 0}}{\Omega_\alpha}\right| \ll 1 \quad (8)$$

where $\Omega_\alpha = q_{\alpha 0}B_0/m_\alpha$ are the different gyrofrequencies. Up to second order in the small quantities we find from equation (5) that

$$\mathbf{u}_{e1} = \frac{\omega-ku_{e0}}{\omega B_0}\mathbf{E}_1\times\mathbf{e}_z-m_e\frac{i(\omega-ku_{e0})^2+\gamma_{ed}k(u_{e0}-u_{d0})}{\omega q_e B_0^2}\mathbf{E}_1$$

$$\mathbf{u}_{i1} = \frac{\omega-ku_{i0}}{\omega B_0}\mathbf{E}_1\times\mathbf{e}_z-m_i\frac{i(\omega-ku_{i0})^2+\gamma_{id}k(u_{i0}-u_{d0})}{\omega q_i B_0^2}\mathbf{E}_1$$

$$\mathbf{u}_{d1} = \frac{\omega-ku_{d0}}{\omega B_0}\mathbf{E}_1\times\mathbf{e}_z$$

$$-m_d \frac{i(\omega - ku_{d0})^2 + k\gamma_{de}(u_{d0}-u_{e0}) + k\gamma_{di}(u_{d0}-u_{i0})}{\omega q_{d0} B_0^2} \mathbf{E}_1 \quad (9)$$

and with the help of equations (6) and (7) obtain the following linear dispersion relation

$$(\omega - k\bar{U})^2 - k^2(V_A^2 - W) + ik\Gamma = 0. \quad (10)$$

In this V_A is the global Alfvén velocity defined through

$$V_A^2 = \frac{B_0^2}{\mu_0(\rho_{e0}+\rho_{i0}+\rho_{d0})} \quad (11)$$

where $\rho_{\alpha 0} = m_\alpha n_{\alpha 0}$, $\bar{U}$ is the bulk mass velocity of the whole plasma, including the charged dust

$$\bar{U} = \frac{\rho_{e0}u_{e0}+\rho_{i0}u_{i0}+\rho_{d0}u_{d0}}{\rho_{e0}+\rho_{i0}+\rho_{d0}} \quad (12)$$

and the combined charging and streaming effects occur in

$$\Gamma = \frac{(\rho_{e0}\gamma_{ed} - \rho_{d0}\gamma_{de})(u_{d0}-u_{e0}) + (\rho_{i0}\gamma_{id} - \rho_{d0}\gamma_{di})(u_{d0}-u_{i0})}{\rho_{e0}+\rho_{i0}+\rho_{d0}}. \quad (13)$$

Since the dust grains typically have a much lower charge-to-mass ratio than ordinary protons, the Alfvén velocity V_A is much smaller than usual. In addition, W refers to the mass averaged relative kinetic energy in the parallel flows, given by

$$W = \frac{\rho_{e0}\rho_{i0}(u_{e0}-u_{i0})^2 + \rho_{e0}\rho_{d0}(u_{e0}-u_{d0})^2 + \rho_{i0}\rho_{d0}(u_{i0}-u_{d0})^2}{(\rho_{e0}+\rho_{i0}+\rho_{d0})^2}. \quad (14)$$

The square root of W could then serve as a measure for the normalized average drift velocity. The effect of the dust charge fluctuations drops out of the linear dispersion relation (10). This is owing to the fact that, like density fluctuations, the dust charge fluctuations give rise to first-order current perturbations in the $\mathbf{e}_z$ direction, which do not couple to the transverse waves considered here as a consequence of our using a deHoffmann–Teller frame.

4. Analysis and results

The solution of equation (10) is given by

$$\omega = \left[k\bar{U} \mp \left(\frac{(A^2+k^2\Gamma^2)^{1/2}+A}{2}\right)^{1/2}\right] \pm i\left(\frac{(A^2+k^2\Gamma^2)^{1/2}-A}{2}\right)^{1/2} \quad (15)$$

where $A = k^2(V_A^2 - W)$.

4.1. *Case I with* $\Gamma = 0$

If the charging effects conserve momentum between any two species, as true collisional effects usually do, then

$$\rho_{e0}\gamma_{ed} = \rho_{d0}\gamma_{de}, \quad \rho_{i0}\gamma_{id} = \rho_{d0}\gamma_{di} \quad (16)$$

and Γ vanishes exactly.

For $\Gamma = 0$ and $W > V_A^2$, A becomes negative and equation (15) yields the dispersion relation

$$\omega = k\bar{U} + ik\sqrt{(W - V_A^2)}. \quad (17)$$

For $Zm_e/m_d \ll m_e/m_i \ll 1$ expressions (11), (12) and (14) are simplified to

$$\bar{U} = \frac{u_{i0}+\sigma u_{d0}}{1+\sigma}, \quad W = \frac{\sigma(u_{i0}-u_{d0})^2}{(1+\sigma)^2} \quad (18)$$

and

$$V_A^2 = \frac{B_0^2}{\mu_0\rho_{i0}\left(1+\dfrac{\rho_{d0}}{\rho_{i0}}\right)} = \frac{V_{Ai}^2}{1+\sigma} \quad (19)$$

where V_{Ai} is the Alfvén velocity with respect to the mass of the ion beams and $\sigma = \rho_{d0}/\rho_{i0}$ is the ratio of the mass densities of dust particles and ions. The condition $W > V_A^2$ then demands that instability would occur provided the relative Alfvén Mach number $M = |u_{i0}-u_{d0}|/V_{Ai} > M_{cr}$, where the critical Mach number is given by $M_{cr} = (1+1/\sigma)^{1/2}$.

Coming back to the conditions of validity (8) of our dispersion relation, with Ω_d being by far the smallest of all the gyrofrequencies in absolute value and the frequency becoming complex, we need for the moduli that

$$|\omega - ku_{d0}|^2 = |\mathrm{Re}\,\omega - ku_{d0}|^2 + |\mathrm{Im}\,\omega|^2 \ll \Omega_d^2. \quad (20)$$

Working this out, with the help of equations (17)–(19) and the definition of M, gives the allowable range of wave numbers as

$$k \ll \frac{|\Omega_d| M_{cr}}{V_{Ai}} \cdot \sqrt{\left(\frac{\sigma}{M^2-1}\right)}. \quad (21)$$

At the same time, one can compute that the growth rate will peak for a given Mach number for those relative densities obeying

$$\sigma_m = \frac{M^2+1}{M^2-1} > \frac{1}{M^2-1} = \sigma_{cr}. \quad (22)$$

Here σ_{cr} stands for the minimum value needed to obtain instability. It is now simple to see that at this maximum growth rate for a given M

$$|\mathrm{Re}\,\omega - ku_{d0}| = |\mathrm{Im}\,\omega| = kV_{Ai}\frac{M^2-1}{2M}. \quad (23)$$

For most of the practical applications, however, σ, the ratio of the mass densities of dust particles and protons, is a rather large number compared with 1 and therefore equation (23) is not of much help in the case of dusty plasmas. From equation (17) we obtain, in an inertial

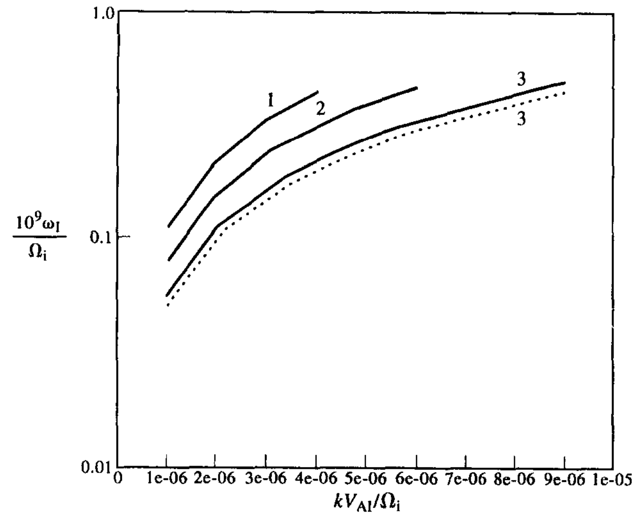

Fig. 1. Variation of growth rates and real frequencies normalized by the proton gyrofrequency versus the normalized wave number, kV_{Ai}/Ω_i, and for $M = 1.2599$, $\sigma = 4.783\times10^7$, 9.566×10^7, and 19.132×10^7 for curves 1, 2 and 3, respectively. Here as well as in the remainder of the figures the solid and the dotted curves represent growth rates and real frequencies respectively (Case I)

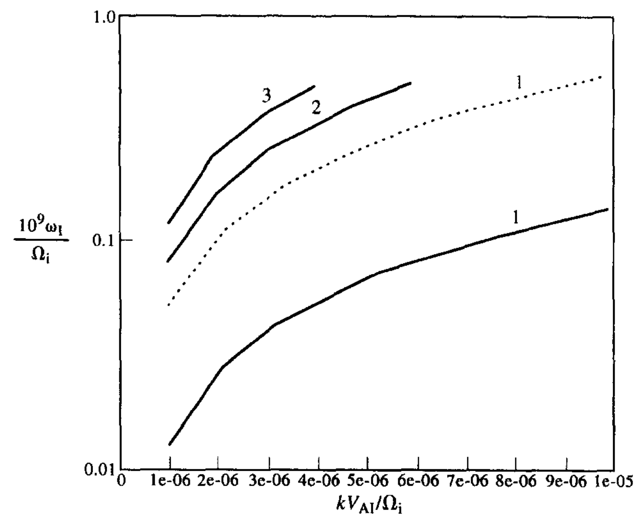

Fig. 2. Same as Fig. 1 for $\sigma = 9.566\times10^7$, $M = 1.0079$, 1.2599 and 1.5119 for curves 1, 2 and 3, respectively (Case I)

frame where the dust has a small streaming velocity, approximate expressions for large σ as:

$$\mathrm{Re}\,\omega \simeq \frac{kV_{Ai}M}{\sigma}, \quad \mathrm{Im}\,\omega = \frac{kV_{Ai}}{M_{cr}^2}\sqrt{\left(\frac{M^2-M_{cr}^2}{\sigma}\right)}. \tag{24}$$

It is readily seen that $\mathrm{Im}\,\omega$ increases with M and decreases with σ. Conversely from equation (21), the allowed k increases with σ, so that finally, at given M, the growth rates and the wavelengths $\lambda = 2\pi/k$ of the structures both decrease with σ.

Once k obeys equation (21), it is usually the case that for the ions and the electrons the conditions that

$$|\mathrm{Re}\,\omega - ku_{i0,e0}|^2 + |\mathrm{Im}\,\omega|^2 \ll \Omega_{i,e}^2 \tag{25}$$

are also satisfied. Hence the biggest constraint upon the wave numbers is the one coming from the small dust gyrofrequencies.

These conclusions have been borne out by some numerical computations, the results of which are shown in Figs 1 and 2, where the variation of the real frequency (dotted curve) and the growth rates (solid curves), normalized by Ω_i, are given versus kV_{Ai}/Ω_i, the normalized wave number. In all figures, the different parameters have been fixed according to the equilibrium relationships (4). We notice from Fig. 1 that the growth rates indeed decrease with increasing σ (cf. solid curves 1, 2 and 3). Also the growth rate and the real frequency increase with the normalized wave number, the range of which increases as σ increases.

Figure 2 shows that increasing the Mach number M results in an increase in growth rates and the shift of unstable wave numbers to lower values of k (cf. curves 1, 2 and 3). For $M \leqslant M_{cr}$, the dispersion relation (15) yields stable modes.

4.2. *Case II where* $\Gamma \neq 0$

When the charging and discharging effects do not conserve momentum between any two species in the sense of equation (16), then $\Gamma \neq 0$. Unlike true collisions where momentum is exchanged by changes in the velocities of the colliding particles, here momentum is exchanged by shifting charges from the electron and ion fluids to the dust and vice versa. Therefore, it would not seem necessary for the dust to behave so as to make Γ vanish exactly, but more complicated three-way processes might be involved. As a zeroth-order approximation we consider all charging frequencies to be constant.

For $\Gamma \neq 0$, we find that for the case of $M > M_{cr}$, the effect of Γ is negligible on the modes considered here. However, the effect of finite Γ is significant for $W \leqslant V_A^2$ or $M \leqslant M_{cr}$, which we discuss below. For simplicity we shall consider again $Zm_e/m_d \ll m_e/m_i \ll 1$, and now also $\gamma_{di} \simeq \gamma_{de} \simeq 0$. Then equation (13) is approximately

$$\Gamma = \frac{\gamma_{id}(u_{d0}-u_{i0})}{1+\sigma}. \tag{26}$$

4.2.1. *Case II.A when* $W < V_A^2$. For $W < V_A^2$ or $M < M_{cr}$, and in the limit $A^2 \gg k^2\Gamma^2$, equation (15) simplifies to

$$\omega = \frac{kV_{Ai}}{M_{cr}^2}\left(\frac{M}{\sigma} + \frac{u_{d0}M_{cr}^2}{V_{Ai}} - \sqrt{\left(\frac{M_{cr}^2-M^2}{\sigma}\right)}\right) + \mathrm{i}\frac{\gamma_{id}M}{2\sqrt{(\sigma(M_{cr}^2-M^2))}}. \tag{27}$$

The different assumptions made in deriving the above equation demand that the following inequalities are satisfied:

$$\frac{M_{cr}^2 M}{M_{cr}^2-M^2}\cdot\frac{\gamma_{id}}{|\Omega_d|} \ll \frac{kV_{Ai}}{|\Omega_d|} \ll M_{cr}^2\sqrt{\left(\frac{\sigma}{M_{cr}^2-M^2}\right)}. \tag{28}$$

The condition on the growth rate is then automatically fulfilled.

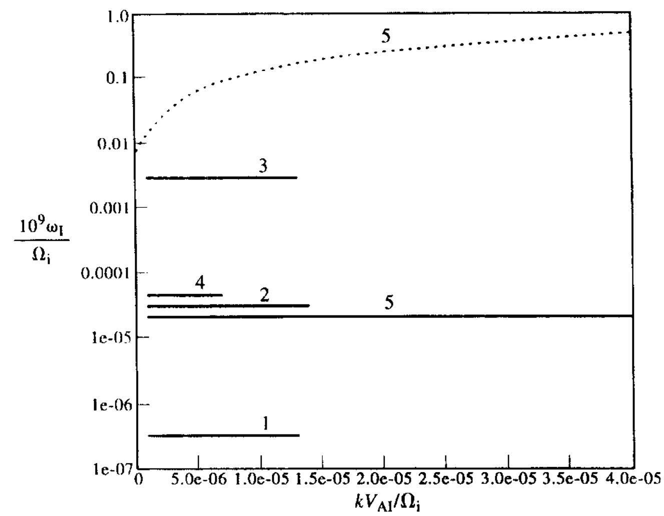

Fig. 3. Same as Fig. 1 for $\sigma = 9.566 \times 10^7$, $M = 0.504$ and for $\gamma_{id} = 10^{-11}\Omega_i$, $10^{-9}\Omega_i$ and $10^{-7}\Omega_i$ for curves 1, 2 and 3, respectively. For curves 4 and 5, $\gamma_{id} = 10^{-9}\Omega_i$, and $\sigma = 4.783 \times 10^7$ and 19.132×10^7, respectively (Case II.A). Here and in Figs 4 and 5, the dotted curves show the magnitude of the real frequencies which are found to be negative

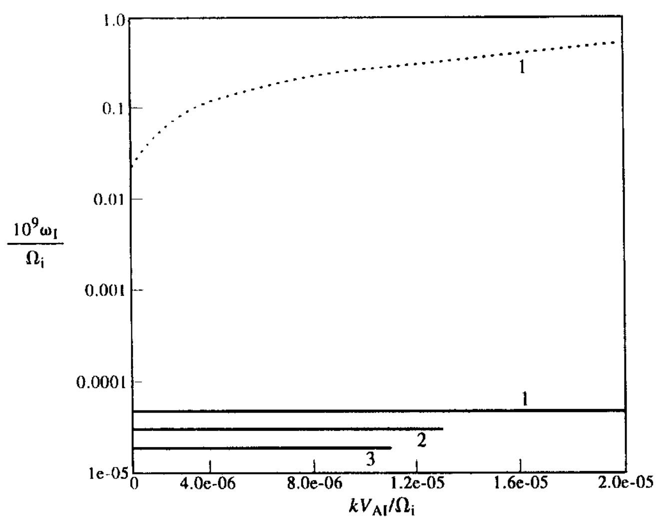

Fig. 4. Same as Fig. 1, but for $\sigma = 9.566 \times 10^7$, $\gamma_{id} = 10^{-9}\Omega_i$, and for $M = 0.672$, 0.504 and 0.336 for curves 1, 2, and 3, respectively (Case II.A)

Similarly to Case I, we have shown in Figs 3 and 4, the variation of the real frequency (dotted curve) and the growth rates (solid curves) normalized by Ω_i versus kV_{Ai}/Ω_i, the normalized wave number. From Figs 3 and 4 we notice that the growth rates are nearly constant, whereas the real frequencies increase with increasing normalized wave number. Figure 3 shows that the growth rates increase by an increase in γ_{id} (cf. solid curves 1, 2 and 3). The effect of increasing σ results in the decrease of the growth rates and the increase of unstable wave numbers (cf. solid curves 4, 2, and 5). From Fig. 4 it is seen that an increase in the relative Mach numbers M is destabilizing for this mode (cf. solid curves 1, 2, and 3).

4.2.2. *Case II.B when* $W = V_A^2$. When $W = V_A^2$ or $M = M_{cr}$, the dispersion relation (15) reduces to

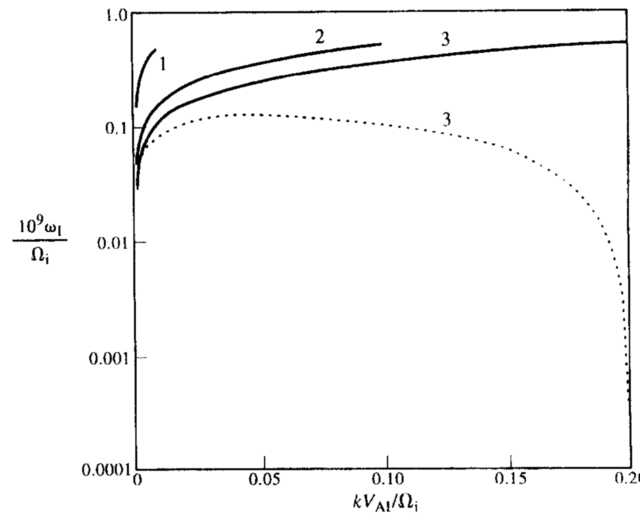

Fig. 5. Same as Fig. 1, but for $\sigma = 1.993 \times 10^8$, and for $\gamma_{id} = 10^{-8}\Omega_i$ and $10^{-9}\Omega_i$ for curves 1 and 2, respectively. Curve 3 is for $\gamma_{id} = 10^{-9}\Omega_i$ and $\sigma = 3.986 \times 10^8$ (Case II.B)

$$\omega = \left\{ kV_{Ai}\left(\frac{1}{\sigma M_{cr}} + \frac{u_{d0}}{V_{Ai}} + \right) - \sqrt{\left(\frac{kV_{Ai}\gamma_{id}}{2\sigma M_{cr}}\right)} \right\} + i\sqrt{\left(\frac{kV_{Ai}\gamma_{id}}{2\sigma M_{cr}}\right)}. \quad (29)$$

The conditions for the validity of our assumptions leading to equation (29) are met provided

$$kV_{Ai} \ll \frac{\sigma M_{cr}\Omega_d^2}{\gamma_{id}} \quad (30)$$

allowing for larger k and hence smaller structures than in the previous cases. This is borne out by our computations, which show in Fig. 5 the variation of the real frequency (dotted curves) and the growth rates (solid curves), normalized with Ω_i versus kV_{Ai}/Ω_i, the normalized wave number. From equation (27), it is seen that when $M = 0$, the unstable modes disappear, whereas of course in equation (29) $M = M_{cr} > 0$. However, for $\gamma_{id} = 0$, the modes described by equations (27) and (29) reduce to stable Alfvén type modes. Hence for the modes to grow, both $M \neq 0$ and $\gamma_{id} \neq 0$ are necessary. These properties are similar to those of drift dissipative modes where density gradients give rise to negative energy modes which grow owing to collisional dissipation. Here the role of a density gradient drift is replaced by the relative streaming between ion and dust beams.

5. Conclusions

Our analysis shows that nonresonant, low-frequency, long-wavelength electromagnetic modes can grow in multi-beam dusty plasmas when the momentum loss of electrons and ions owing to fluctuations in the dust grain charges is taken into account. We apply our results to the case of cometary environments where typically the dust grain size is a few microns and the dust material mass density is about 10^3 kg m^{-3}. The typical ratio of proton to dust gyrofrequencies is $\Omega_i/\Omega_d = m_d/Zm_i \simeq 0.6 \times 10^9$ for an equilibrium charge on the dust grains of the order of $Z = 10^3$. We shall consider a magnetic field of $B_0 = 8$ nT, which gives $\Omega_i/2\pi = 0.12$ Hz and $\Omega_d/2\pi = 0.2 \times 10^{-9}$ Hz.

From Figs 1 and 2 we find that for the case of $\Gamma = 0$ (Case I), the real frequency is $\mathrm{Re}\,\omega \simeq (0.03-0.3)\Omega_d$, and the growth rate $\mathrm{Im}\,\omega \simeq (0.005-0.3)\Omega_d$. For the case of $\Gamma \neq 0$ (Case II), Figs 3–5 give $|\mathrm{Re}\,\omega| \simeq (0.0006-0.3)\Omega_d$ and $\mathrm{Im}\,\omega \simeq (0.2 \times 10^{-6}-0.3)\Omega_d$.

Figures 1–4 predict the range of unstable wave numbers to be $k \simeq (10^{-6}–10^{-5})(\Omega_i/V_{Ai}) \simeq (0.44–4.4) \times 10^{-14} n_{i0}^{1/2}$ m$^{1/2}$. For $n_{i0} = 10^9$ m^{-3}, which can be considered as typical inside the cometopause (Mendis and Horanyi, 1991), the unstable wavelengths become $\lambda = 2\pi/k \simeq (45.0–4.5) \times 10^6$ km. However, from Fig. 5, which corresponds to the special case of $M = M_{cr}$ (Case II.B), we get unstable wave numbers with $k \simeq (0.001–0.2)(\Omega_i/V_{Ai})$. This can give rise to $\lambda \simeq (4.5–0.2) \times 10^3$ km. The shortest scalelengths produced by these unstable modes would be of the order of 200 km.

Our analysis cannot be applied directly to dusty environments of the rings of Jupiter and Saturn, as we would expect the planetary magnetic fieldlines from a nearly perfectly aligned dipole to be perpendicular to the equatorial plane in which the bulk of the ring material can move. Hence there would be no relative streaming along the field in a deHoffmann–Teller frame. However, for oblique rotators as Uranus and Neptune, where the magnetic and rotation axes are not parallel at all, our analysis might have some relevance. Moreover, the frequencies of the unstable modes will change depending on the magnetic field, dust mass and dust charge. Since the unstable wave numbers scale as $n_{i0}^{1/2}$, as shown above, we expect the shortest wavelengths produced by these unstable modes to be $\sim$200 km in a planetary environment. Hence the unstable modes considered here are capable of generating spatial structures of the order of 200 km–45 million km in dusty cometary tails and in the planetary rings of Uranus and Neptune.

Acknowledgments. FV thanks the (Belgian) National Fund for Scientific Research for a research grant. For PM this text presents research results of a program initiated by the Belgian State, Prime Minister's Office and the Federal Office for Scientific, Technical and Cultural Affairs. We are grateful to Drs J. Lemaire and M. Roth for many interesting discussions.

References

Bhatt, J. R. and Pandey, B. P., Self-consistent charge dynamics and collective modes in a dusty plasma. *Phys. Rev. E* **50,** 3980–3983, 1994.

Booker, H. G., *Cold Plasma Waves*, p. 7. Martinus Nijhoff, Dordrecht, 1984.

D'Angelo, N., Ion-acoustic waves in dusty plasmas. *Planet. Space Sci.* **42,** 507–511, 1994.

de Angelis, U., Formisano, V. and Giordano, M., Ion plasma waves in dusty plasmas: Halley's comet. *J. Plasma Phys.* **40,** 399–406, 1988.

Draine, B. T. and Salpeter, E. E., On the physics of dust grains in hot gas. *Astrophys. J.* **231,** 77–94, 1979.

Galeev, A. A., Sagdeev, R. Z., Shapiro, V. D., Shevchenko, V. I. and Szegö, K., Quasilinear theory of the ion cyclotron instability and its application to the cometary plasma, in *Cometary Plasma Processes* (edited by A. D. Johnstone), Geophysical Monograph Series 61, pp. 223–240. AGU, Washington, 1991.

Gary, S. P. and Winske, D., Computer simulations of electromagnetic instabilities in the plasma sheet boundary layer. *J. geophys. Res.* **95,** 8085–8094, 1990.

Goertz, C. K., Dusty plasmas in the solar system. *Rev. Geophys.* **27,** 271–292, 1989.

Havnes, O., A streaming instability interaction between the solar wind and cometary dust. *Astron. Astrophys.* **193,** 309–312, 1988.

Jana, M. R., Sen, A. and Kaw, P. K., Collective effects due to charge-fluctuation dynamics in a dusty plasma. *Phys. Rev. E* **48,** 3930–3933, 1993.

Lakhina, G. S., Low-frequency plasma turbulence during solar wind–comet interaction. *Astrophys. Space Sci.* **133,** 203–218, 1987.

Lakhina, G. S. and Verheest, F., Alfvén wave instabilities and ring current during solar wind–comet interaction. *Astrophys. Space Sci.* **143,** 329–338, 1988.

Li, F., Havnes, O. and Melandsø, F., Longitudinal waves in a dusty plasma. *Planet. Space Sci.* **42,** 401–407, 1994.

Melandsø, F., Aslaksen, T. K. and Havnes, O., A new damping effect for the dust-acoustic wave. *Planet. Space Sci.* **41,** 321–325, 1993a.

Melandsø, F., Aslaksen, T. K. and Havnes, O., A kinetic model for dust acoustic waves applied to planetary rings. *J. geophys. Res.* **98,** 13315–13323, 1993b.

Mendis, D. A. and Horanyi, M., Dust–plasma interactions in the cometary environment, in *Cometary Plasma Processes* (edited by A. D. Johnstone), Geophysical Monograph Series 61, pp. 17–25. AGU, Washington, 1991.

Mendis, D. A. and Rosenberg, M., Cosmic dusty plasma. *A. Rev. Astron. Astrophys.* **32,** 419–463, 1994.

Pilipp, W., Hartquist, T. W., Havnes, O. and Morfill, G. E., The effects of dust on the propagation and dissipation of Alfvén waves in interstellar clouds. *Astrophys. J.* **314,** 341–351, 1987.

Rao, N. N., Low-frequency waves in magnetized dusty plasmas. *J. Plasma Phys.* **49,** 375–393, 1993.

Rao, N. N., Shukla, P. K. and Yu, M. Y., Dust-acoustic waves in dusty plasmas. *Planet. Space Sci.* **38,** 543–546, 1990.

Shukla, P. K., Low-frequency modes in dusty plasmas. *Physica Scripta* **45,** 504–507, 1992.

Shukla, P. K. and Stenflo, L., Stimulated scattering of electromagnetic waves in dusty plasmas. *Astrophys. Space Sci.* **190,** 23–32, 1992.

Shukla, P. K., Yu, M. Y. and Bharuthram, R., Linear and nonlinear dust drift waves. *J. geophys. Res.* **96,** 21343–21346, 1991.

Spitzer Jr, L., *Physical Processes in the Interstellar Medium.* Wiley, New York, 1978.

Varma, R. K., Shukla, P. K. and Krishan, V., Electrostatic oscillations in the presence of grain-charge perturbations in dusty plasmas. *Phys. Rev. E* **47,** 3612–3616, 1993.

Verheest, F., Alfvén wave plasma turbulence during solar wind–comet interaction. *Astrophys. Space Sci.* **138,** 165–173, 1987.

Verheest, F., Nonlinear dust-acoustic waves in multispecies dusty plasmas. *Planet. Space Sci.* **40,** 1–6, 1992a.

Verheest, F., Parallel solitary Alfvén waves in warm multi-species beam-plasma systems. Part 2. Anisotropic pressures. *J. Plasma Phys.* **47,** 25–37, 1992b.

Verheest, F., Nonlinear dust Alfvén modes. *Space Sci. Rev.* **68,** 109–114, 1994.

Verheest, F. and Buti, B., Parallel solitary Alfvén waves in warm multi-species beam-plasma systems. Part 1. *J. Plasma Phys.* **47,** 15–24, 1992.

Verheest, F. and Lakhina, G. S., Nonresonant low-frequency instabilities in multibeam plasmas: applications to cometary environments and plasma sheet boundary layers. *J. geophys. Res.* **96,** 7905–7910, 1991.

Verheest, F. and Meuris, P., Whistler-like instabilities due to charge fluctuations in dusty plasmas. *Phys. Lett. A* **198,** 228–232, 1995.